

# Improving the triaxial bulge model of M31

Simon Berman<sup>1</sup><sup>★</sup> and Laurent Loinard<sup>2</sup>

<sup>1</sup>*Theoretical Physics, University of Oxford, 1 Keble Road, Oxford OX1 3RH*

<sup>2</sup>*Instituto de Astronomía, Universidad Nacional Autónoma de México, Apartado Postal 72-3, 58089 Morelia, Michoacán, México*

Accepted 2002 June 7. Received 2002 May 24; in original form 2001 December 11

## ABSTRACT

A detailed hydrodynamical model of the gas flow in the triaxial gravitational potential of the bulge of the Andromeda galaxy (M31) has recently been proposed by Berman, and shown to provide excellent agreement with the CO emission-line velocities observed along its major axis. In the present paper, we confirm the validity of that model by showing that it can also reproduce the CO velocities observed off the major axis – a much more robust test. The CO observations, however, tend to span a wider range of velocities than a direct application of the original model of Berman would suggest. This situation can be improved significantly if the molecular disc is made thicker, a requirement already encountered in dynamical simulations of other spiral galaxies, and typically attributed to a broadening of the molecular layer in galactic fountain-like processes. In the central regions of M31, however, it is unclear whether there actually is a thick molecular disc, or whether broadening the molecular layer is merely an artificial theoretical means of accounting for some disc warping. Other effects not included in the model, such as hydraulic jumps, might also contribute to a widening of the range of velocities.

**Key words:** hydrodynamics – galaxies: bulges – galaxies: evolution – galaxies: individual: M31 – galaxies: ISM – galaxies: structure.

## 1 INTRODUCTION

There is growing evidence that spiral galaxies, in which no bar is easily seen on optical or infrared images, none the less have triaxial bulges. Twisting of the inner isophotes and misalignments between the disc and the bulge major axes (both of which have been detected in several spirals with no obvious bar) are clear signposts of triaxiality. Even stronger cases have been made by combining optical or infrared photometric data with spectroscopic observations of the gaseous interstellar component. Indeed, when submitted to a triaxial gravitational potential, the interstellar gas near the centre of a spiral galaxy can be found at higher velocities than expected from circular motion. Such anomalous velocities have been reported in several galaxies where no strong bar is visible, including the two nearest examples: the Milky Way (Rougoor & Oort 1959; Dame, Hartmann & Thaddeus 2001) and the Andromeda galaxy (Lindblad 1956; Loinard et al. 1999).

The triaxiality of spiral galaxy bulges is particularly important for two reasons. First, it can affect the dynamics of interstellar gas, gathering large amounts of it near galactic centres. This could help to explain the appearance of active galactic nuclei. On long time-scales, a buildup of gas in galactic centres could affect the morphology of spiral galaxies, and imply secular changes in their Hubble types. Secondly, triaxiality allows more constraints to be derived from

spectral observations. In an axisymmetric system, the rotation curve only allows the determination of the radial mass distribution, without providing any three-dimensional information. In particular, it is not possible to assess in an axisymmetric system whether the dark matter component is distributed in a flat disc-like structure or in a spherical halo. In a triaxial system, that disc–halo degeneracy can be removed, with obviously important consequences for our understanding of dark matter. Cold dark matter (CDM) models, for instance, favour spherical haloes.

Since triaxiality primarily affects the dynamics at the centres of spiral galaxies, it should be sought in our neighbours, where the achievable linear resolution is highest. This is particularly important when using radio observations of the gaseous component, which often have limited angular resolution. Detailed studies of the dynamics of the central regions of the Milky Way are adversely affected by our location inside the system, and the well-known associated confusion and distance ambiguity problems. However, the existence of triaxial features in the inner Galaxy has been postulated for over 40 years. Based on the discovery of the 3-kpc arm, Kerr (1967) proposed the existence of a gaseous bar at the Galactic Centre, and Mulder & Liem (1986) modelled the arm as a density wave in a barred potential. By combining photometric and kinematic data, Gerhard & Vietri (1986) demonstrated the triaxiality of the Galactic bulge, and *COBE* images of the Galactic Centre have confirmed this triaxiality (Dwek et al. 1995; Binney, Gerhard & Spergel 1997).

The next nearest spiral (the Andromeda Galaxy – M31) has no clear visible bar, and is an excellent target for a dynamical study,

<sup>★</sup>E-mail: simon@thphys.ox.ac.uk

because its high inclination enables an accurate determination of the gas kinematics. M31 has long been known to have twisted inner isophotes and misaligned bulge and disc major axes (Lindblad 1956). Moreover, the existence of anomalous gas velocities in the inner few kiloparsecs is also now well established for both the atomic (Brinks & Burton 1984) and molecular (Loinard et al. 1996, 1999) components. A convincing interpretation in terms of triaxiality was put forward as early as 1956 by Lindblad, and was further developed by Stark (1977) and Stark & Binney (1994). However, those early works were hampered by the lack of strong observational constraints.

The distribution and kinematics of the atomic component of the interstellar medium (ISM) have long been known at high resolution and sensitivity across the entire disc of M31 thanks to interferometric observations of the 21-cm line of atomic hydrogen (Brinks & Shane 1984, and references therein). However, those observations do not provide clear information on the ISM kinematics in central regions, because the kinematic component associated with the warped outer disc can be seen in projection through the inner disc. The resulting confusion between inner and outer discs seen in the H I position–velocity diagrams of the central regions of M31 precludes accurate studies of its dynamics. The molecular component traced by CO emission is a better tracer of the dynamics of the inner regions because no CO emission can be detected in the warped outer disc. However, the inner regions of M31 are also particularly dim in CO (Dame et al. 1993; Loinard et al. 1999). Fragmentary CO observations of the central regions of M31 were used to constrain the model of Stark & Binney (1994). Recently, however, more systematic CO observations have been obtained.

Loinard, Allen & Lequeux (1995) presented a deep search for CO emission along the inner major axis of M31. This search confirmed the existence of anomalous velocities in the inner few kiloparsecs of M31, and results along the line of nodes of the disc were used by Berman (2001) to constrain an improved dynamical model of the central regions of M31 (see Section 2 below). However, Berman (2001) pointed out that off-axis CO observations would provide better constraints. Such data are now available – at least for the southern half of M31 – thanks to the CO(1–0) survey made at the Five College Radio Astronomy Observatory (FCRAO; Loinard et al. 1996, 1999). The angular resolution of the survey is  $\sim 1$  arcmin, and it covers the entire southern part of M31 with a sampling of 50 arcsec. The observational noise level is nearly constant across the entire surveyed region, with a typical rms of 45–50 mK per 3.25 km s<sup>-1</sup> spectral channel. Although the CO(1–0) is found to peak in the broad Population I ring at 10 kpc from the centre, significant emission is still detected in the inner 2–3 kpc (10–15 arcmin), where most constraints can be obtained about the triaxiality of the bulge. The integrated intensity images or position–velocity diagrams shown by Loinard et al. (1999), as well as the position–velocity diagrams that will be shown in this paper, have been obtained after ‘unsharp masking’ was applied to the data. In this scheme, a data cube smoothed in both position and velocity (but not regridded) is first constructed from the original data. The average noise level  $\sigma$  in this smoothed cube is computed, and all the pixels in the non-smoothed data cube where no significant ( $> 3\sigma$ ) emission is found in the smoothed version are blanked. This avoids unnecessary noise being added when summations over several pixels are performed, and in effect reduces the noise in integrated maps by a factor of a few. A slight drawback of this method is that the noise becomes dependent on the number of pixels summed (or averaged), and therefore on the position in the maps.

Anomalous velocities are clearly seen in this data set in the inner regions of M31 (see fig. 12 in Loinard et al. 1999). While the cut along the major axis essentially shows the same anomalous velocities as reported by Loinard et al. (1995), cuts parallel to the major axis provide new constraints for the models, as called for by Berman (2001).

## 2 ORIGINAL MODEL

The dynamical model developed by Berman (2001) takes into account a rotating, triaxial bulge, and an axisymmetric component that mimics the combined influence of the disc and halo. The properties of the bulge are obtained by finding a triaxial mass distribution which gives the observed  $R^{1/4}$   $B$ -band surface brightness profile when rotated and inclined to the plane of the sky. Properties of the axisymmetric component are deduced from a simple interpretation of H I and CO kinematics. The gas response to the gravitational potential is computed using a hydrodynamical code (GALAHAD) that solves the non-self-gravitating, isothermal Euler equations, on a regular Cartesian grid, using the FS2 algorithm of van Albada, van Leer & Roberts (1982). Each grid cell is 125 pc (37.5 arcsec) on a side, which is similar to the resolution ( $\sim 60$  arcsec) of the CO data. Removal and injection of interstellar matter by star formation and stellar mass loss respectively are included (somewhat crudely) in the algorithm.

Berman (2001) constrained the parameters of his model by comparing the output gas flow with the CO observations along the line of nodes of the disc of M31 of Loinard et al. (1995). The best fit to the data is obtained for a bulge semi-major axis  $a = 3.5$  kpc, a pattern speed  $\Omega_p = 53.7$  km s<sup>-1</sup> kpc<sup>-1</sup>, a corotation radius to bulge semi-major axis ratio  $\mathcal{R} = 1.2$ , an angle  $\phi$  between the major axis of the bulge and the disc line of nodes of  $15^\circ$ , and a bulge mass-to-light ratio  $\Upsilon_B = 6.5$ . This in turn implies a bulge mass<sup>1</sup> of  $M_{\text{bulge}} = 2.3 \times 10^{10} M_\odot$ . The disc mass within the radius of the bulge (3.5 kpc) can be estimated by assuming reasonable values for the  $B$ -band exponential disc central surface brightness ( $I_0 = 21.6$  mag arcsec<sup>-1</sup>; Walterbos & Kennicutt 1988), which when corrected for absorption and inclination using the values of Berman (2001) gives a central surface density of  $\Sigma_d = 113 L_\odot \text{pc}^{-3}$ , a disc scalelength ( $R_d = 5.8$  kpc; Walterbos & Kennicutt 1988), and a conservative disc mass-to-light ratio of 4. This gives a disc mass of  $M_{\text{disc}} = 1.2 \times 10^{10} M_\odot$ . The total (bulge + disc + halo) mass inside the same radius can be estimated from the rotation curve as  $M_{\text{total}} = 3.7 \times 10^{10} M_\odot$ , leaving little room for a dark halo.

The value of  $\mathcal{R} = 1.2$  found by Berman (2001) implies that the bulge of M31 is a fast rotator. Interestingly, of the few galaxies for which  $\mathcal{R}$  has been measured, all have been found to be fast rotators. Debattista & Sellwood (2000) showed that such fast bars cannot coexist with massive dark haloes because dynamical friction would slow them down rapidly. The value of  $\mathcal{R} = 1.2$  is further evidence that M31 must have a minimal halo, and, consequently, a maximum disc. This is notably at odds with the contentions of CDM models, which predict massive haloes and minimal discs (e.g. Navarro, Frenk & White 1997).

## 3 MODELLING OFF-AXIS OBSERVATIONS

As mentioned earlier, Berman (2001) pointed out that a much stronger case could be made for his best-fitting model if it were

<sup>1</sup> The value given for the mass of the bulge in Berman (2001) was not correct. The amended version has been used in this paper.

found to be consistent with observations of CO velocities away from the line of nodes of the disc. Moreover, it is important to utilize these off-axis velocities since dynamical models of the bulge of M31 have never before been constrained by real 3D  $(X, Y, V)$  observations.

To compare accurately the output of the model with the data, we performed a 2D convolution of the model with a realistic description of the FCRAO beam, consisting of the sum of a sinc function and two Gaussians. The sidelobes of the sinc function provide a good (very conservative) description of any coma effects, while the two Gaussians describe the response of the FCRAO antenna to emission coming from angles far away from the nominal pointing position, owing to the imperfections of the dish (Ladd & Heyer 1996). The sinc function has a full width at half-maximum (FWHM) of 45 arcsec and the two Gaussians have FWHM and attenuations of 30 arcmin and 30 dB, and  $4^\circ$  and 50 dB, respectively. This convolution produces multiple velocities at each  $X$ -position in the  $(X, V)$  position–velocity diagrams derived from the model, in the same way as multiple velocities arise naturally in the data cube.

Fig. 1 shows position–velocity diagrams for observational data at  $Y = \pm y \times 50$  arcsec, where  $y = 1, 2, 3$ . Overlaid are Berman’s best-fitting model predictions convolved with the FCRAO beam function which should, if the model is correct, approximately enclose the observations on every plot. In this, as in all of the comparisons below, the model has been interpolated to fit the positions of the observations. Although the general trends of the predictions and the observations are similar, the model data enclose a narrower range of velocities than the observations and are further from the systemic velocity than the observations. The discrepancies are just as large or

greater for models with different input parameters. In particular, it is not reasonable to use a smaller rotation velocity. This would help to reconcile the predictions of the model proposed by Berman (2001) with the data in the central regions, but would predict velocities much too small at distances larger than about 40 arcmin from the centre.

The same ‘beard’ phenomenon is seen in the position–velocity diagrams of the spiral galaxy NGC 2403 (fig. 1 of Schaap, Sancisi & Swaters 2000). The arguments presented in that paper conclude that the beard is caused by either a thick high-density gas layer with a half-width at half-maximum (HWHM) intensity of 500 pc, or a lower density layer with a HWHM of 1.75 kpc, rotating more slowly than the standard thin disc. This conclusion is motivated by galactic fountain models (Spitzer 1990) in which hot gas from supernova explosions and galactic winds rises from the disc into the halo. As it rises, the gravitational attraction towards the centre of the galaxy lessens, the gas moves outwards and, by conservation of angular momentum, its azimuthal velocity decreases. Thick molecular discs have been seen in CO in the Milky Way Galaxy (Dame & Thaddeus 1994), and the edge-on spiral galaxy NGC 891 (Garcia-Burillo et al. 1992).

To recover the small magnitude and large range of velocities of the observations of M31, the bulge model of Berman (2001) is augmented by the kinematics of a thick disc which has been rotated and inclined to the observer’s frame. The vertical density distribution follows Schaap et al. (2000) in taking a Gaussian form:

$$\rho(z) = \rho_0 \exp\left(-z^2/2z_0^2\right), \quad (1)$$

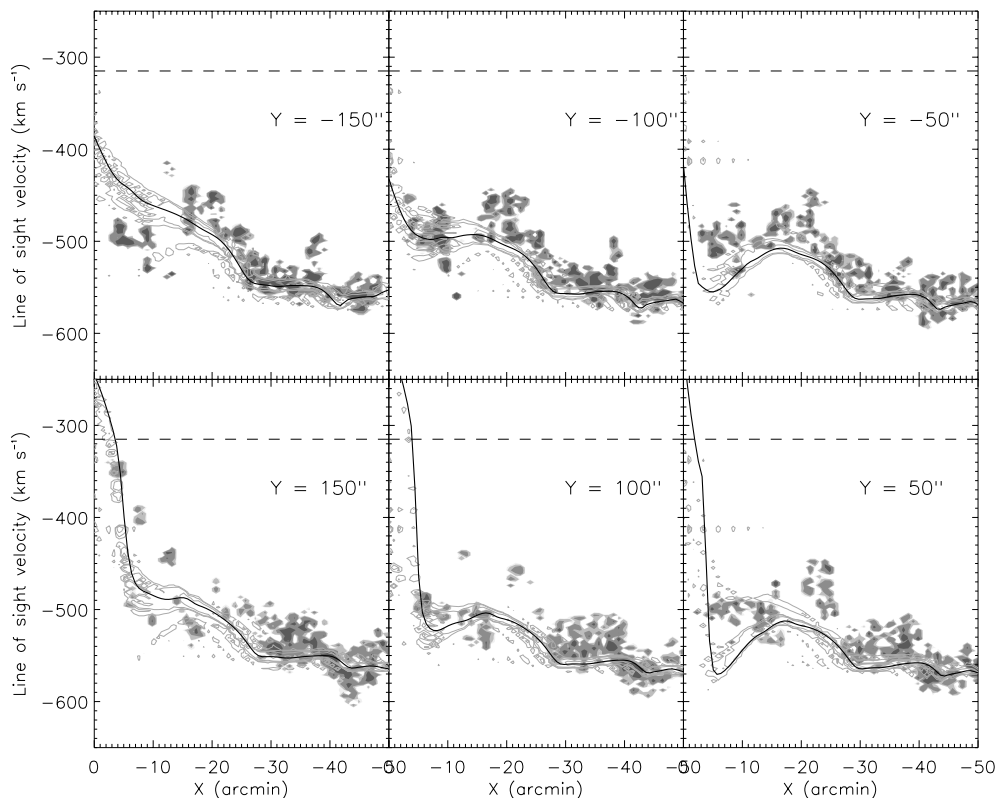


**Figure 1.** Comparison of CO observations and gas velocities from the model of maximum likelihood of Berman (2001) away from the line of nodes of the disc. Model data were convolved with the 2D function representing the FCRAO beam as described in the text. Intensity is plotted as a grey-scale for observations and using contour levels for model data. Contours are given at 1, 3, 10 and 30 per cent of the maximum value in each subplot. The dashed line indicates the systemic velocity and the solid line the results at  $Y$  arcsec ignoring the effects of the thick disc and of the beam function.

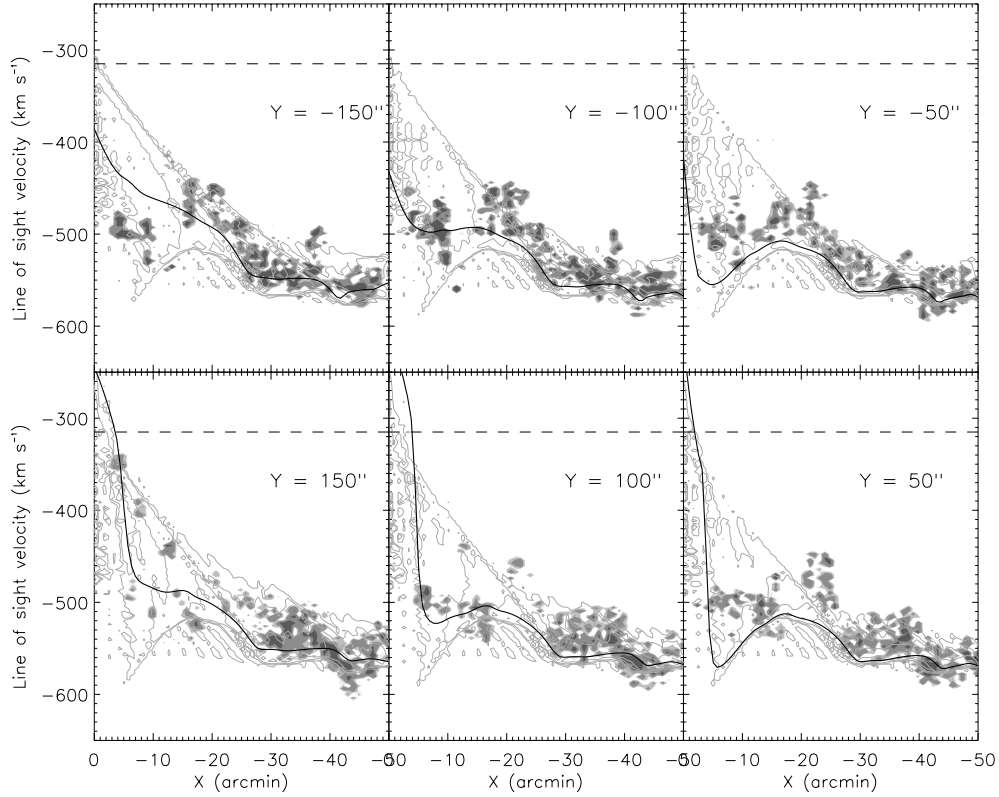


**Figure 2.** Comparison of CO observations and gas velocities from the model of maximum likelihood away from the line of nodes of the disc. The model includes a corotating thick disc of scaleheight  $z_0 = 400$  pc. Model data were convolved with the 2D function representing the FCRAO beam as described in the text. Intensity is plotted as a grey-scale for observations and using contour levels for model data. Contours are given at 1, 3, 10 and 30 per cent of the maximum value in each subplot. The dashed line indicates the systemic velocity and the solid line the results at  $Y$  arcsec ignoring the effects of the thick disc and of the beam function.

$$\rho_0 = \frac{\Sigma_0}{(2\pi)^{1/2} z_0}, \quad (2)$$

where  $\rho_0$  and  $\Sigma_0$  are the density and surface density respectively at  $z = 0$ , and  $z_0$  is the vertical scaleheight of the gas. The HWHM intensity  $z_{1/2} = 1.18z_0$ . The intensities at  $(X, Y)$  are convolved in 2D with the function representing the FCRAO beam as described earlier, to produce position–velocity plots for  $Y = \pm y \times 50$  arcsec, where  $y = 1, 2, 3$ . Fig. 2 compares the observational data with the results from a model with  $z_0 = 400$  pc, the lowest value of the scaleheight that adequately encloses the vast majority of the observations for  $X > -50$  arcmin. For this model,  $z_{1/2} = 472$  pc. This is very large when compared with the thick disc observed by Dame & Thaddeus (1994) in the Milky Way, for which the HWHM is between 71 and 133 pc depending on position, but smaller than the thick disc of NGC 891 (Garcia-Burillo et al. 1992), where the HWHM is larger than 1 kpc.

We now follow Schaap et al. (2000) and drop the implicit assumption that the thick disc is corotating with the  $z = 0$  plane, and reduce the velocities of the gas where  $z \neq 0$ . Velocities parallel to the  $z$ -axis stay fixed at zero. A slow thick disc is implied by the galactic fountain models and was also invoked by Swaters, Sancisi & van der Hulst (1997) to explain the H I observations of NGC 891. We take the linear velocity distribution used in both papers:

$$v(z) = v_0(1 - \gamma z), \quad (3)$$

where  $v_0$  is the velocity in the  $z = 0$  plane,  $\gamma$  is the velocity lost per kpc and  $z$  is the height. By slowing the gas down above and below the

plane of the disc, the range of velocities at a particular scaleheight is extended. It can be seen in Fig. 3 that a similar range of velocities to both the observations and the corotating model is produced if the scaleheight is just 200 pc and  $\gamma = 0.3$ , i.e. the gas loses 30 per cent of its speed per kpc away from the plane of the disc. This implies that  $z_{1/2} = 236$  pc which is closer to but still larger than the values quoted for the Milky Way by Dame & Thaddeus (1994) and much smaller than the value for NGC 891.

By including a thick disc, the model initially proposed by Berman (2001) is able to match the 3D CO data of Loinard et al. (1999) reasonably well. The most noticeable discrepancy is found around  $X = \pm 20$ – $25$  arcmin,  $V \sim -45$  km s $^{-1}$ , a position that the original model found difficult to account for even along the line of nodes of the disc. It is plausible that some vertical or turbulent gas motions not included in our model can account for these remaining discrepancies.

As mentioned above, galactic fountain models are often invoked to account for thick gaseous discs in the centres of galaxies. However, they are probably not justifiable in M31 since it does not harbour a great deal of star formation. Moreover, whilst the thick disc found by Dame & Thaddeus (1994) in the Milky Way appears to be much fainter in CO than the Galactic mid-plane, the present modelling requires that in M31 it be just as bright. A plausible alternative follows from the recent work by Martos & Cox (1998), who describe many numerical simulations combining magnetic fields with hydrodynamics to create post-shock regions in which large pressure gradients exist near to the mid-plane, causing the gas layer to expand vertically. The result is a ‘hydraulic jump’ in which a buildup of gas

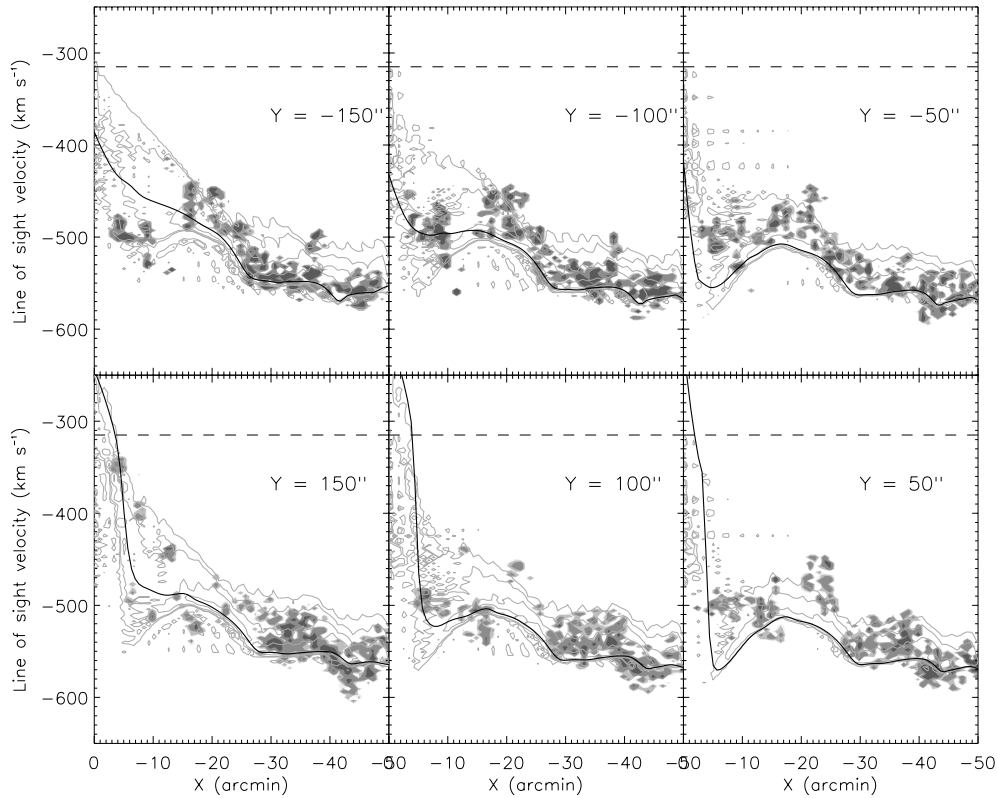


**Figure 3.** Comparison of CO observations and gas velocities from the model of maximum likelihood away from the line of nodes of the disc. The model includes a thick disc of scaleheight  $z_0 = 200$  pc and a loss of velocity of  $0.3v_0 \text{ kpc}^{-1}$  away from the plane of the disc. Model data were convolved with the 2D function representing the FCRAO beam as described in the text. Intensity is plotted as a grey-scale for observations and using contour levels for model data. Contours are given at 1, 3, 10 and 30 per cent of the maximum value in each subplot. The dashed line indicates the systemic velocity and the solid line the results at  $Y$  arcsec ignoring the effects of the thick disc and of the beam function.

in the vertical direction can be seen with scaleheights of hundreds of parsecs.

Another, perhaps more controversial, possibility should be mentioned here. Pringle, Allen & Lubow (2001) contend that much of the ISM in spiral galaxies is molecular, but too cold to be easily detectable in CO. In this view, only the parts of molecular clouds illuminated by newly formed stars are bright in CO. The CO-bright thin disc could then correspond to the thin layer where stars form most actively, whereas the thick disc would correspond to the real total extent of the molecular layer. The existence of large quantities of cold molecular gas in the inner regions of M31 has been proposed by Loinard & Allen (1998, and references therein). Moreover, since the inner region of M31 harbours little star-forming activity, the thin disc there would not be particularly brighter in CO than the thick disc, and the distinction between the two would indeed vanish.

Finally, a last possibility is that the inner disc of M31 is actually thin, but warped. Modelling it as a thick disc then becomes a convenient way to account for the gas located in the warped parts of the disc, above or below the mid-plane.

#### 4 CONCLUSIONS

In this paper, we show that hydrodynamical triaxial models of the bulge of the Andromeda galaxy (M31) previously presented by Berman (2001), and initially tested against CO emission observations along the apparent major axis only, can also account for the CO emission velocities observed off the apparent major axis – a

much more robust validity test. The triaxial model implies that the bulge of M31 is a fast rotator and hence the dark matter contained in its central regions must be minimal and coincident with the stellar disc.

To account for the whole velocity range covered by the observations, a finite, fairly large thickness (HWHM intensity of 200–500 pc) must be given to the molecular disc. It is quite unclear, however, whether the inner molecular disc of M31 is truly that thick or whether adding it to the model is merely an effective theoretical trick that is able to account for a warping of a thinner disc. Other out-of-plane or peculiar velocities (such as those associated with hydraulic jumps or turbulence) could also contribute to the wide velocity range covered by the CO observations.

#### ACKNOWLEDGMENTS

We thank James Binney and Daniel Pfenniger for careful reading of the manuscript, and interesting comments.

#### REFERENCES

- Berman S., 2001, *A&A*, 371, 476
- Binney J. J., Gerhard O. E., Spergel D., 1997, *MNRAS*, 288, 365
- Brinks E., Burton W. B., 1984, *A&A*, 141, 195
- Brinks E., Shane W. W., 1984, *A&AS*, 55, 179
- Dame T. M., Thaddeus P., 1994, *ApJ*, 436, L173
- Dame T. M., Koper E., Israel F. P., Thaddeus P., 1993, *ApJ*, 418, 730
- Dame T. M., Hartmann D., Thaddeus P., 2001, *ApJ*, 547, 792

- Debattista V. P., Sellwood J. A., 2000, *ApJ*, 543, 704  
Dwek E. et al., 1995, *ApJ*, 445, 716  
Garcia-Burillo S., Guélin M., Cernicharo J., Dahlem M., 1992, *A&A*, 266, 21  
Gerhard O. E., Vietri M., 1986, *MNRAS*, 223, 377  
Kerr F. J., 1967, in van Woerden H., ed., *Proc. IAU Symp. 31, Radio Astronomy and the Galactic System*. Academic Press, London, p. 239  
Ladd N., Heyer M. H., 1996, *FCRAO Technical Memorandum*  
Lindblad B., 1956, *Stockholm Obs. Annal.*, 2  
Loinard L., Allen R. J., 1998, *ApJ*, 499, 227  
Loinard L., Allen R. J., Lequeux J., 1995, *A&A*, 301, 68  
Loinard L., Dame T. M., Koper E., Lequeux J., Thaddeus P., Young J. S., 1996, *ApJ*, 469, L101  
Loinard L., Dame T. M., Heyer M. H., Lequeux J., Thaddeus P., 1999, *A&A*, 351, 1087  
Martos M. A., Cox D. P., 1998, *ApJ*, 509, 713  
Mulder W. A., Liem B. T., 1986, *A&A*, 157, 148  
Navarro J. F., Frenk C. S., White S. D. M., 1997, *ApJ*, 490, 493  
Pringle J. E., Allen R. J., Lubow S. H., 2001, *MNRAS*, 327, 663  
Rougoor G. W., Oort J. H., 1959, in Bracewell R. N., ed., *Proc. IAU Symp. 9, Paris Symposium on Radio Astronomy*. Stanford Univ. Press, Stanford, CA, p. 416  
Schaap W. E., Sancisi R., Swaters R. A., 2000, *A&A*, 356, 49  
Spitzer L., Jr, 1990, *ARA&A*, 28, 71  
Stark A. A., 1977, *ApJ*, 213, 368  
Stark A. A., Binney J., 1994, *ApJ*, 426, 31  
Swaters R. A., Sancisi R., van der Hulst J. M., 1997, *ApJ*, 491, 140  
van Albada G. D., van Leer B., Roberts W. W., 1982, *ApJ*, 108, 76  
Walterbos R. A. M., Kennicutt R. C., 1988, *A&A*, 198, 61

This paper has been typeset from a  $\text{\TeX}/\text{\LaTeX}$  file prepared by the author.